Transition temperature of strong-coupled superconductors reanalyzed

P. B. Allen*
Department of Physics, State University of New York, Stony Brook, New York 11790

R. C. Dynes
Bell Laboratories, Murray Hill, New Jersey 07974

(Received 20 January 1975)

A thorough analysis is made of the dependence of the superconducting transition temperature T_c on material properties (λ, μ^*, phonon spectrum) as contained in Eliashberg theory. The most striking new feature of the analysis is in the asymptotic regime of very large λ where T_c is found to equal $0.15(\lambda\langle\omega^2\rangle)^{1/2}$ (assuming $\mu^* = 0.1$). This result implies the surprising conclusion that within Eliashberg theory T_c is not limited by the phonon frequencies, and also shows that McMillan's "$\lambda = 2$ limit" is spurious. The McMillan equation (with a prefactor altered from $\Theta_D/1.45$ to $\omega_{\log}/1.2$) is found to be highly accurate for all known materials with $\lambda < 1.5$ but in error for large values of λ. Correction factors to McMillan's equation are found in terms of λ, μ^*, and one additional parameter, $(\langle\omega^2\rangle)^{1/2}/\omega_{\log}$. The frequency $\omega_{\log}$ is defined as $\exp\langle\ln\omega\rangle$ where the averages $\langle\ln\omega\rangle$ and $\langle\omega^2\rangle$ are defined using $(2/\lambda\omega)\alpha^2F(\omega)$ as a weight factor. These conclusions are based on a combination of analytic and numerical solutions of the Eliashberg equations, and are supported by a comparison with tunneling data. Especially strong support comes from a new experimental result for amorphous $Pb_{0.45}Bi_{0.55}$ reported herein. This material has parameters $\lambda = 2.59$ and $T_c/\omega_{\log} = 0.284$, in serious disagreement with McMillan's formula but in good agreement when the correction factors are included. The McMillan-Hopfield parameter η [or $N(0)\langle I^2\rangle$] is extracted from tunneling measurements or from a combination of empirical values of λ and neutron-scattering measurements of phonon dispersion. It is proposed that η (which is now known not to be accurately constant) is the most significant single parameter in understanding the origin of high T_c and the limitation of T_c by colvalent instabilities.

I. INTRODUCTION

The most extensive study of the relation between microscopic theory and observed superconducting transition temperature T_c was made by McMillan.[1] In the subsequent seven years there has been a significant accumulation of microscopic information on strong-coupling superconductors coming most notably from tunneling experiments but also from inelastic neutron scattering, electron spectroscopy, and energy-band theory. In this paper, McMillan's work is reexamined in the light of this new information. We find several aspects of his work which agreed well with information available at the time on medium-coupling superconductors ($0.5 < \lambda < 1$) but need modification for strongly coupled materials ($\lambda > 1$) which have been more recently studied. We attempt to make the appropriate modifications.

McMillan's work is based on the Eliashberg equations[2] which are extensions of the original Bardeen-Cooper-Schrieffer (BCS) theory,[3] and were first written in their finite-temperature form by Scalapino, Schrieffer, and Wilkins.[4] The microscopic ingredients of Eliashberg theory are the Coulomb repulsion $\mu = N_\uparrow(0)|V_c|$ [where $N_\uparrow(0)$ is the single-spin density of electronic states at the Fermi surface], and the electron-phonon spectral function $\alpha^2F(\omega)$ defined as

$$\alpha^2F(\omega) = N_\uparrow(0)\frac{\sum_{kk'}|M_{kk'}|^2\delta(\omega-\omega_Q)\delta(\epsilon_k)\delta(\epsilon_{k'})}{\sum_{kk'}\delta(\epsilon_k)\delta(\epsilon_{k'})}, \quad (1)$$

where $\vec{Q}=\vec{k}-\vec{k}'$, ω_Q and ϵ_k are phonon and electron energies, respectively, Q and k run over wave number and band quantum numbers for phonons and electrons, $M_{kk'}$ is the electron-phonon coupling matrix element, and the δ functions restrict the electrons to the Fermi surface. Given these parameters, the zero-temperature Eliashberg theory determines the complex energy-gap function $\Delta(\omega)$, and the finite-temperature Eliasberg theory determines T_c. The quantity $|\Delta(\omega)|^2$ is measureable by quasiparticle tunneling, and McMillan and Rowell[5] have been able to use measured tunneling conductances to determine $\alpha^2F(\omega)$ and μ^* by inverting the zero-temperature Eliashberg theory. The resulting functions $\alpha^2F(\omega)$ tend[6] to have a close similarity to the phonon density of states $F(\omega)$ as deduced from neutron scattering. It is primarily information derived from this technique that has motivated the present work.

The principal content of McMillan's 1968 paper[1] is the solution of the finite-temperature Eliashberg theory to find T_c for various cases, and the construction from this of an approximate equation relating T_c to a small number of simple parameters:

$$T_c = \frac{\langle\omega\rangle}{1.20}\exp\left(-\frac{1.04(1+\lambda)}{\lambda-\mu^*(1+0.62\lambda)}\right). \quad (2)$$

The original McMillan equation contained $\Theta_D/1.45$ instead of $\langle\omega\rangle/1.20$, which was introduced later by

Dynes.[7] The parameter λ is a dimensionless measure of the strength of α^2F:

$$\lambda \equiv 2\int_0^\infty d\omega\, \alpha^2F(\omega)/\omega . \tag{3}$$

The quantity $1+\lambda$ plays the role of an electron mass enhancement and renormalizes certain observables such as the electronic specific heat. In terms of BCS theory, λ corresponds to $N_\sigma(0)|V_{ph}|$. The parameter μ^* is an effective Coulomb repulsion reduced from the instantaneous repulsion μ by the fact that Coulomb coupling is propagated much more rapidly than phonon coupling,

$$\frac{1}{\mu^*} = \frac{1}{\mu} + \ln\left(\frac{\omega_{el}}{\omega_{ph}}\right). \tag{4}$$

The ratio ω_{el}/ω_{ph} is a ratio of propagation times; ω_{el} corresponds to a plasma frequency or a high-frequency peak in $\mathrm{Im}[1/\epsilon(\omega)]$, where $\epsilon(\omega)$ is the dielectric function, while ω_{ph} corresponds to the high-frequency cutoff in $\alpha^2F(\omega)$. A time lag occurs in the electron pairing which is the source of both the frequency dependence of $\Delta(\omega)$ and the reduction of the effective Coulomb repulsion. Finally, $\langle\omega\rangle$ is the first moment of the normalized weight function $g(\omega) = (2/\lambda\omega)\alpha^2F(\omega)$, where the general moment is defined as

$$\langle\omega^n\rangle = \frac{2}{\lambda}\int d\omega\, \alpha^2F(\omega)\,\omega^{n-1} . \tag{5}$$

The principal content of the present paper is a more extensive set of numerical solutions for T_c at larger values of the coupling parameter λ than were studied by McMillan, and for a variety of shapes of the weight function $g(\omega)$. We find that McMillan's Eq. (2) underestimates T_c for large values of λ, and also underestimates the extent to which T_c depends on the shape of $g(\omega)$.

The plan of this paper is as follows: In Sec. II, the mathematical apparatus used in solving for T_c is discussed. The asymptotic behavior of T_c at large λ is rigorously shown to be $\sim(\lambda\langle\omega^2\rangle)^{1/2}$ rather than $\sim\langle\omega\rangle$ as in Eq. (2). The numerical results are summarized in Sec. III, where it is shown that the shape dependence of T_c is described (for $\lambda<2$) if the prefactor $\langle\omega\rangle$ of Eq. (2) is replaced by a logarithmic average frequency, equal to the $n\to 0$ limit of the sequence of average frequencies

$$\bar{\omega}_n \equiv \langle\omega^n\rangle^{1/n} . \tag{6}$$

In Sec. IV the available tunneling data are summarized and a new experiment is reported for a very-strong-coupling system, amorphous Pb-Bi, which provides strong confirmation of our calculations in the large-λ region. In Sec. V a new approximate T_c equation is presented which consists of correction factors to McMillan's Eq. (2). In Sec. VI the question of causes of and limitations to high T_c's is discussed. The McMillan "$\lambda=2$ limit" is shown to be spurious. Data on high-T_c materials are analyzed and it is concluded that the parameter $\eta = \lambda M\langle\omega^2\rangle$ is of crucial importance in raising T_c. The "covalent instabilities" which appear to limit η are discussed. Appendix A presents some mathematical analysis used in Sec. II, and Appendix B discusses the asymptotic limit of BCS theory. The principal results of Secs. I–V have already been published in a short note.[8]

II. MATHEMATICAL ANALYSIS

The value of T_c is determined from the interaction parameters $\alpha^2F(\omega)$ and μ^* via the Eliashberg equations. Because the gap $\Delta(\omega)$ vanishes at T_c, this becomes a linear equation for the infinitesimal function $\Delta(\omega)$. The condition that a nonzero solution exists determines the value of T_c. Two equivalent versions of this equation have been used: a mathematically direct matrix equation[9,10] for $\Delta(i\omega_n)$ on the Matsubara imaginary-frequency points $\omega_n = (2n+1)\pi T$; or a physically meaningful integral equation for $\Delta(\omega)$ on the real-frequency domain, obtained from the former by analytic continuation.[4] McMillan's analysis[1] was based on this latter version, and has the advantage that physical insight can be brought to bear. In particular, the solution $\Delta(\omega)$ at T_c bears a close resemblance to the measureable gap function at low temperatures. However, the kernel of the integral equation is made complicated by the occurrence of poles on the real axis and various unwieldy combinations of Fermi and Bose factors. A recent analysis of this kernel by Kessel[11] has confirmed the results of McMillan's numerical analysis under the assumption that the Bose factors are negligible. Less sophisticated analyses by Allen[12] and by Leavens[13] indicate that the Bose factors are not negligible in every instance. These mathematical difficulties are avoided by remaining at the imaginary-frequency points, where poles do not occur and statistical occupation factors disappear. An additional benefit for computer programming is the occurrence of an exact discrete matrix representation, which eliminates the practical necessity of constructing an approximate discretization to solve the integral equation.

The Matsubara representation of the gap equation has been discussed by Owen and Scalapino[9] and Bergmann and Rainer.[10] We choose, for our starting point, Eq. (7) of the latter authors,

$$\rho\bar{\Delta}(i\omega_n) = \sum_{m=-N-1}^{N}\left(\lambda(n-m) - \mu^*(N) - \frac{\delta_{m\eta}|\tilde{\omega}_n|}{\pi T}\right) \times \bar{\Delta}(i\omega_m) . \tag{7}$$

In this equation, $\bar{\Delta}$ is a modified gap parameter which becomes $\Delta/|\omega|$ in the limit when the "pair-breaking parameter" ρ (to be discussed shortly)

vanishes:

$$\bar{\Delta}(i\omega_n)=\frac{|\tilde{\omega}_n/\omega_n|\,\Delta(i\omega_n)}{|\tilde{\omega}_n|+\pi T\rho}\,. \tag{8}$$

The frequency $\tilde{\omega}_n$ is ω_n multiplied by $Z(i\omega_n)$, which is the "renormalization function" $Z(\omega)$ of strong-coupling theory[4] evaluated at the Matsubara frequencies:

$$\tilde{\omega}_n=\omega_n Z(i\omega_n)=\omega_n+\pi T\left(\lambda(0)+2\sum_{l=1}^{n}\lambda(l)\right). \tag{9}$$

The interaction parameters $\lambda(n)$ and $\mu^*(N)$ are defined by

$$\lambda(n)=2\int_0^\infty d\omega\frac{\alpha^2F(\omega)\omega}{\omega^2+(2\pi nT)^2}\,, \tag{10}$$

$$\frac{1}{\mu^*(N)}=\frac{1}{\mu}+\ln\left(\frac{\omega_{e1}}{\omega_N}\right). \tag{11}$$

The function $\lambda(n)$ takes the value $\lambda(0)=\lambda$ when $n=0$, using the definition (10).

The integer N must be chosen large enough that the largest eigenvalue ρ is not affected by the choice of N. This is satisfied provided $\lambda(N)$ is much smaller than unity or $\lambda(0)$. We find that satisfactory convergence is obtained provided ω_N exceeds $\sim 8\bar{\omega}_2$, where $\bar{\omega}_2=\langle\omega^2\rangle^{1/2}$ was defined in Sec. I. The parameter $\mu^*(N)$ is the (generally reduced) value of the Coulomb parameter μ which reproduces at cutoff ω_N the effect that μ has at cutoff ω_{e1}. A two-square-well analysis (such as McMillan's) provides an approximate T_c equation, which depends on a number μ^*, which is scaled to a cutoff at some upper phonon frequency ω_{ph} as in Eq. (4). There is no known unique best choice for ω_{ph}, and we have used $\bar{\omega}_2$ in our numerical solutions:

$$\frac{1}{\mu^*}=\frac{1}{\mu}+\ln\left(\frac{\omega_{e1}}{\bar{\omega}_2}\right). \tag{12}$$

It is this number (rather than μ) which has to come be regarded as physically significant, and which is frequently deduced from tunneling experiments or isotope-effect measurements. Therefore, the definition (11) of $\mu^*(N)$ in terms of μ should be rewritten in terms of μ^*:

$$\frac{1}{\mu^*(N)}=\frac{1}{\mu^*}+\ln\left(\frac{\bar{\omega}_2}{\omega_N}\right). \tag{13}$$

It is convenient to make a further simplification of Eq. (7) which follows from the symmetry of the kernel under replacement of ω_i by $-\omega_i$ (i.e., the transformation $n\to -n-1$, $m\to -m-1$). It follows that the eigenfunctions of Eq. (7) must be either even or odd under this transformation, and we can restrict attention to even solutions (odd solutions would be gapless). Then we can write Eq. (7) as

$$\sum_{n=0}^{N}(K_{mn}-\rho\delta_{mn})\Delta_n=0\quad(m\geq 0)\,, \tag{14}$$

$$K_{mn}=\lambda(m-n)+\lambda(m+n+1)-2\mu^*(N)$$
$$-\delta_{mn}\left(2m+1+\lambda(0)+2\sum_{l=1}^{m}\lambda(l)\right), \tag{15}$$

where Δ_n is shorthand for $\bar{\Delta}(i\omega_n)$.

The pair-breaking parameter ρ has so far not been discussed. The physical-gap equation is actually only the special case of (7) or (14) where $\rho=0$. The parameter ρ was introduced by Bergmann and Rainer[10] (we have introduced a scale factor πT) in order to create a standard Hermitian eigenvalue problem, and it is only a convenient mathematical device. At very high temperatures, the eigenvalues of $\underline{K}$ [Eq. (14)] are all negative. If μ^* equals zero, they are approximately the negative odd integers. This can be seen by noting that at large T, $\lambda(n)$ [Eq. (10)] reduces to

$$\lambda(n)\approx\lambda\langle\omega^2\rangle/(2\pi nT)^2 \tag{16}$$

provided $n\neq 0$, $2\pi nT\gg\langle\omega^2\rangle^{1/2}$. Thus $\lambda(n)$ can be made as small as desired by raising the temperature. The exceptional case $\lambda(0)$ cancels with itself and doesn't appear in Eq. (15). As the temperature is lowered toward T_c, one of the eigenvalues ρ begins increasing toward zero, T_c being defined as the temperature at which the first eigenvalue crosses zero. Presumably at still lower temperatures, other eigenvalues could cross zero, but Owen and Scalapino[9] have not found this to happen for a variety of realistic kernels. It is helpful to note that to find T_c we need only study the behavior of the *maximum* eigenvalue ρ_{max}. This eigenvalue is bounded below by the expectation value of the operator $\underline{K}$ taken with any arbitrary trial vector $\vec{\Delta}_t$.

$$\rho_{max}\geq\vec{\Delta}_t\cdot\underline{K}\cdot\vec{\Delta}_t/(\vec{\Delta}_t\cdot\vec{\Delta}_t)=\rho_t\,. \tag{17}$$

(The same inequality is the basis for the Rayleigh-Schrödinger variational procedure for the ground-state energy.) This inequality can be immediately used to generate lower bounds T_{ct} on T_c, by solving $\rho_t(T_{ct})=0$. Provided a solution exists, it is clear that $T_c\geq T_{ct}$. Thus we have a variational condition on the transition temperature, namely, that the actual gap function $\Delta(\omega)$ maximizes T_c. This is an intuitively obvious consequence of the principle that the gap function minimizes the free energy.

Let us now construct the simplest possible trial solution, $\Delta_0=\delta_{n0}$. The corresponding estimate of ρ is

$$\rho_{max}>\rho_0=K_{00}=\lambda(1)-2\mu^*(N)-1. \tag{18}$$

If we evaluate (18) at the actual transition temperature, the inequality (17) tells us that $\rho_0\leq\rho_{max}(T_c)=0$, giving the following rigorous inequality for T_c:

$$2\int_0^\infty d\omega \frac{\alpha^2F(\omega)\omega}{\omega^2+(2\pi T_c)^2} \leq 1+2\mu^*(N). \tag{19}$$

It is convenient at this point to introduce an Einstein model for the spectrum α^2F,

$$\alpha^2F_E(\omega)=\lambda\omega_E\delta(\omega-\omega_E)/2. \tag{20}$$

In Sec. III we will see that the transition temperatures of many real superconductors such as Pb or Nb are only weakly affected by deviations of α^2F from this form. Using the Einstein model, we can solve (19) to get a direct inequality on T_c:

$$T_c \geqq T_{c0}=\frac{\omega_E}{2\pi}\left(\frac{\lambda}{1+2\mu^*(N)}-1\right)^{1/2}. \tag{21}$$

We have immediately the surprising result that if λ is very large, T_c scales at least as fast as $\lambda^{1/2}$ rather than saturating as occurs in the BCS or McMillan formulas. This means that the electron-phonon mechanism does *not* imply a restriction of the type $T_c<\Theta_D$, but can *in principle* lead to an *arbitrarily large* T_c. With this information in mind, it can be seen that in the limit of very large λ, the asymptotic limit of the T_c equation is

$$T_c \to (\lambda\langle\omega^2\rangle)^{1/2} f(\mu^*(N)), \tag{22}$$

where f is a function of μ^* only. This follows because in the large-λ limit [using Eq. (16)], information about T_c, λ, and phonons only enters Eq. (15) in the combination $\lambda\langle\omega^2\rangle/T_c^2$.

We can obtain an improved estimate of T_c by allowing $\vec{\Delta}_t$ to have two components corresponding to $n=0$ and 1. The best choice of such a two-component vector is obtained by diagonalizing the 2×2 matrix $\underline{K}_2$, which consists of the matrix K_{mn} truncated after $n=1$, $m=1$. The large of the two eigenvalues is

$$\begin{aligned}\rho>\rho_1=&-\tfrac{1}{2}[4+4\mu^*(N)+\lambda(1)-\lambda(3)]\\&+\{\tfrac{1}{4}[2+3\lambda(1)-\lambda(3)]^2\\&\quad+[\lambda(1)+\lambda(2)-2\mu^*(N)]^2\}^{1/2}.\end{aligned} \tag{23}$$

From this we can generate an explicit lower bound on T_c analogous to (19) or (21). However, the formulas are complicated and uninstructive. In the limit of large T_c and $\mu^*=0$, the inequality on T_c coming from (23) is

$$T_c \geq T_{c1}=0.180\,(\lambda\langle\omega^2\rangle)^{1/2} \quad (\lambda>10,\ \mu^*=0). \tag{24}$$

The exact behavior in this limit, [14] as deduced from computer calculations with $N+1=64$, is

$$T_c=0.182\,(\lambda\langle\omega^2\rangle)^{1/2} \quad (\lambda\gtrsim10,\ \mu^*=0). \tag{25}$$

Thus the 2×2 approximation has converged to within 1% at large λ.

The eigenvalue ρ can be regarded as depending on T, λ, μ^*, and $g(\omega)$, where $g(\omega)=2\alpha^2F(\omega)/\lambda\omega$ is the normalized spectral function. The procedure described so far consists of solving the equations

$$\rho_n(T_{cn},\lambda,\mu^*,g)=0, \quad n=0,1,\ldots,N \tag{26}$$

obtaining an increasing series $(T_{c0}, T_{c1}, \ldots)$ of lower bounds on T_c. For numerical purposes it is much simpler to regard T_c as fixed and solve instead

$$\rho_n(T_c,\lambda_n,\mu^*,g)=0, \quad n=0,1,\ldots,N \tag{27}$$

obtaining a decreasing series of upper bounds $(\lambda_0, \lambda_1, \ldots)$ on λ. Equation (27) is equivalent to solving the matrix equation

$$\det\underline{K}_n=0=\det(\underline{A}_n+\lambda_n\underline{B}_n), \tag{28}$$

where $\underline{A}_n$ contains the terms of $\underline{K}_n$ which are independent of $\alpha^2F(\omega)$, and $\lambda_n\underline{B}_n$ contains the terms which are linear in $\alpha^2F(\omega)$. In principle one needs to be careful to find the smallest positive eigenvalue λ_n of Eq. (22), but in practice, only one positive eigenvalue seems to occur. [9] We have constructed a computer program[15] which solves for λ_n by inverse iteration, and also finds the corresponding eigenvector $\vec{\Delta}_n$. The matrix size is then doubled, and the previous eigenvector is used as the trial vector in the next iteration loop. The total time required to solve for λ (with a maximum matrix dimension of 64) is less than 1 sec on an IBM 370 computer.

When μ^* vanishes, this procedure converges very rapidly and can be terminated when ω_n is in the range 5 to 10 times $\bar{\omega}_2$. When μ^* is nonvanishing, the nature of the matrix $\underline{K}$ is altered in that the off-diagonal elements no longer fall off as $|n-m|$ increases. This gives a series $(\lambda_0, \lambda_1, \ldots, \lambda_M)$ which never converges in a strict sense unless M is made to exceed the predetermined cutoff N (in which case the Coulomb terms are put to zero for $|n-m|>N$). However, it is possible to obtain a convergent series of approximations by the legitimate procedure of using $\mu^*(n)$ rather than $\mu^*(N)$ in the truncated-matrix solution. If this is done, the series $(\lambda_0, \lambda_1, \ldots)$ rapidly converges. However, the convergence is no longer monotonic, and inequalities of the type (18) and (23) are no longer rigorously true.

In summary, the results of this section provide a rapid computer algorithm for solving the Eliashberg equations for T_c, and the unexpected result that for large λ, T_c behaves as $(\lambda\langle\omega^2\rangle)^{1/2}$. The particular combination $\lambda\langle\omega^2\rangle$ is an interesting one, as McMillan has shown that this product depends only on electronic properties and atomic masses, and is independent of specific features of the lattice dynamics. We will have more to say about this in Sec. VI. It is interesting to note that BCS theory (nonretarded) has an asymptotic form $T_c \to \lambda\Theta_D/2$ for large λ. This is discussed in Appendix B. As a final mathematical observation, it is interesting to ask what is the optimum shape for the function

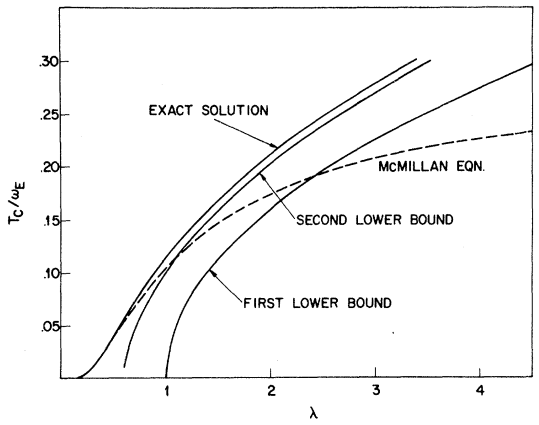

FIG. 1. Calculations for an Einstein spectrum of T_c normalized to the Einstein frequency ω_E as a function of λ for $\mu^* = 0$. The curves labeled first lower bound and second lower bound are from Eqs. (21) and (23) and consist of solving Eq. (14) with N equal to 0 and 1, respectively. The curve labeled "exact solution" was found by solving Eq. (14) with $N = 63$. Deviations from McMillan's equation are apparent when T_c/ω_E exceeds 0.1.

α^2F in the sense that T_c is maximized under the conditions of fixed λ, μ^*, and $\langle\omega^2\rangle$. The asymptotic formula (22) indicates that at very large λ, the shape doesn't affect T_c. At smaller values of λ the shape does play a role. It is clear from inspection of Eq. (15) that the eigenvalue ρ (and thus T_c) is maximized by making the parameters $\lambda(n)$ as large as possible. If we write $\lambda(n)$ in terms of the normalized spectral function $g(\omega)$,

$$\lambda(n) = \lambda \int_0^\infty d\omega \, \frac{g(\omega)\omega^2}{\omega^2 + (2\pi n T)^2} , \qquad (29)$$

we can then ask which shape of $g(\omega)$ (for fixed second moment $\langle\omega^2\rangle$) maximizes $\lambda(n)/\lambda$. It is proved in Appendix A that the Einstein spectrum optimizes the integral (29) and thus is the preferred phonon spectrum.

III. NUMERICAL RESULTS

In Sec. II, the mathematical basis for our computer solutions of the Eliashberg equations has been described. In this section we present numerical results and compare them with tunneling experiments.

The simplest case is the idealized model of an Einstein phonon spectrum with no Coulomb repulsion ($\mu^* = 0$). For this case the first two lower bounds on T_c are simple enough to be solved analytically, and they are shown in Fig. 1. These lower bounds are of no help if λ is small because the lower bounds vanish. The curve in Fig. 1 labeled "exact solution" is actually the 64th lower bound. As mentioned previously, the second lower bound has converged to within 1% of the exact T_c for $\lambda > 10$, and we believe that the 64th lower bound has converged to within 1% for $\lambda > 0.3$ (and $\mu^* = 0$). In the range $0.3 < \lambda < 1.5$, the calculated T_c's agree very well with McMillan's functional form[1] $e^{-1.04(1+\lambda)/\lambda}$. This is illustrated more clearly in Fig. 2, where the logarithm of T_c is plotted versus $(1+\lambda)/\lambda$. There is in fact a slight displacement toward higher T_c's in our calculations at small λ which corresponds to a 5% increase in the prefactor of the exponential and arises from the fact that the Einstein spectrum yields higher T_c's than McMillan's niobium spectrum. For values of λ exceeding 0.5, the exact solutions shown in Fig. 1 begin to depart from McMillan's equation, and the departure becomes significant for $\lambda > 1$. If a positive value of μ^* is used, the departure from McMillan's equation is postponed to larger λ, but occurs always for T_c/ω exceeding 0.1. It is perhaps surprising that this effect was not seen in McMillan's original calculations. The explanation is that McMillan calculated only cases where T_c/ω did not exceed 0.1. In Fig. 2 it can be seen that on a scale of $(1+\lambda)/\lambda$, the departure from McMillan's equation is confined to a narrow range between 1 and 1.75, which was omitted in McMillan's work. A strong hint of this deviation was found by Leavens and Carbotte.[16]

The predicted asymptotic behavior of T_c as $\lambda^{1/2}$

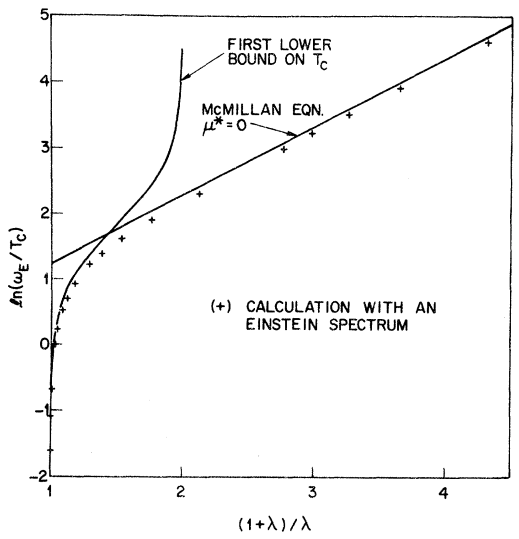

FIG. 2. Logarithm of ω_E/T_c versus $(1+\lambda)/\lambda$ calculated for an Einstein spectrum with $\mu^* = 0$. McMillan's equation is also shown, and agrees well with the calculations at large values of $(1+\lambda)/\lambda$. At small values the calculations suddenly deviate from the straight line in a fashion dictated by the first lower bound, Eq. (21). This graph is similar to McMillan's Fig. 1 (Ref. 1) except that McMillan included only values of $(1+\lambda)/\lambda$ greater than 2, and used a slightly different phonon spectrum which accounts for a slight displacement.

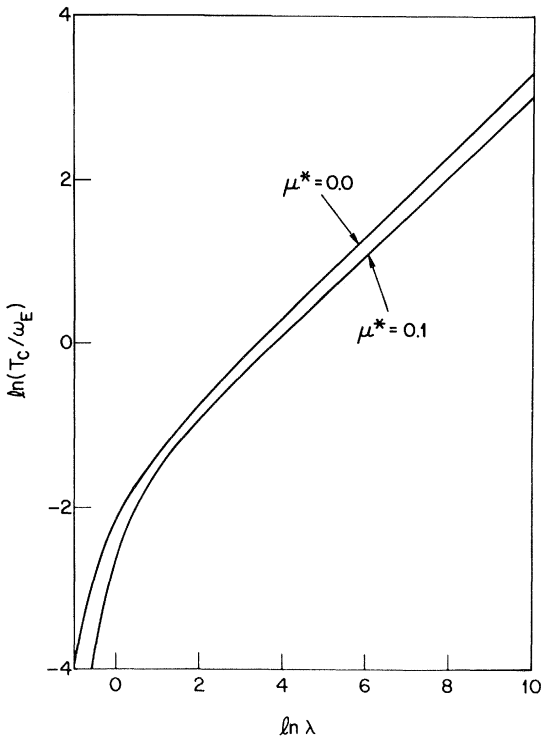

FIG. 3. A log-log plot of T_c/ω_E vs λ calculated for an Einstein spectrum. The slope at large λ is 0.5. The asymptotic formulas for T_c/ω_E are $0.18\lambda^{1/2}$ and $0.15\lambda^{1/2}$ for $\mu^*=0$ and 0.1, respectively.

is verified by a log–log plot in Fig. 3. For values $\lambda \geq 10$, which corresponds to $T_c \geq 0.6\ \omega_E$, the asymptotic formulas $0.18\,\omega_E\,\lambda^{1/2}$ for $\mu^*=0$ and $0.15\ \omega_E\,\lambda^{1/2}$ for $\mu^*=0.1$ are good approximations to T_c. As mentioned in Sec. II, these results are independent of the shape of $\alpha^2F(\omega)$ provided T_c is high enough and ω_E is replaced by $(\langle\omega^2\rangle)^{1/2}$. Unfortunately, there are no materials known to have λ greater than 3. However, it is clear that, in principle, if λ could be large enough, T_c can be almost arbitrarily large. However, if $2\pi T_c$ became comparable to the Fermi energy, the validity of the Eliashberg theory would be doubtful because of possible complications related to Migdal's theorem.

An important test of the consistency of the Eliashberg equations is the comparison between measured values of T_c and values computed from the α^2F curves which are extracted from low-temperature tunneling spectra. Because the "measured" α^2F are required to give the observed value of $\Delta(\omega=0)\equiv\Delta_0$, this test consists of calculating the deviation of $2\Delta_0/k_BT_c$ from the BCS value of 3.52. In all cases where we have performed this test the agreement has been excellent, confirming the conclusions of several other workers, especially Swihart,[17] Owen and Scalapino,[9] Bergmann and Rainer,[10] Trofimenkoff and Carbotte,[18] and Leavens.[19] As another test of our computer programs we have repeated McMillan's calculations[1] using the same choice of α^2F which he used to represent niobium. This test is illustrated in Fig. 4. McMillan's results and ours are not completely overlapping because we used a maximum matrix size of 64, which guarantees convergence only when $T_c/\overline{\omega}_2$ exceeds 0.01, whereas McMillan was able to solve for very much smaller values of T_c. In the region where our methods overlap, the agreement is excellent for $\mu^*=0$ but discrepancies of ~ 7% exist at the largest values of μ^*. This discrepancy probably arises from slightly different choices of the phonon cutoff frequency, which occurs in the definition (4) or (12) of μ^*. This in turn produces a slight discrepancy in the size of $\mu^*(N)$ as determined in Eq. (13). Such a discrepancy is negligible for small value of μ^* but becomes noticeable if $\mu^*\sim 0.2$. In general the agreement between these independent calculations is quite satisfactory.

When $T_c/\overline{\omega}_2$ is not very large (i.e., $\lambda<10$), we expect the shape of $\alpha^2F(\omega)$ to play a role in determining T_c. Of the shapes known from tunneling experiments, lead and mercury stand out as in some sense prototypical. The lead spectrum was measured by Rowell and McMillan[20] and has a shape typical of simple crystalline metals. The mercury spectrum was measured by Hubin and Ginsberg[21] and represents an extreme case of wide dispersion

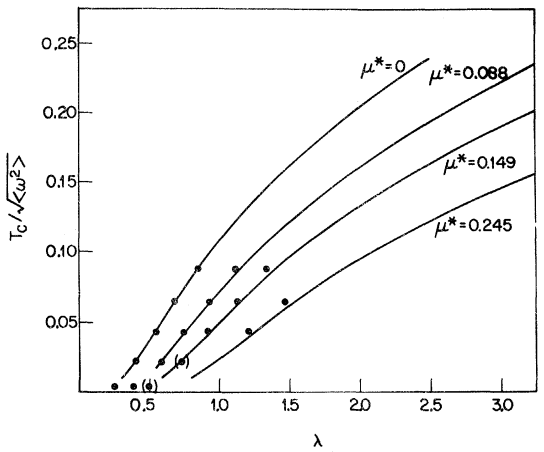

FIG. 4. $T_c/(\langle\omega^2\rangle)^{1/2}$ plotted versus λ. The solid lines are calculated from Eq. (14) using $N=63$, for various values of μ^* and the same shape $\alpha^2F(\omega)$ as used by McMillan to represent niobium. The points are McMillan's calculations as summarized in Table I of Ref. 1. The points enclosed in parentheses have $\mu^*=0.157$, otherwise μ^* is the same as on the nearest labeled line. The agreement between these independent calculations is excellent except for a systematic deviation for large μ^*, which probably derives from a slight difference in the definition of μ^*, which is unimportant if μ^* is small.

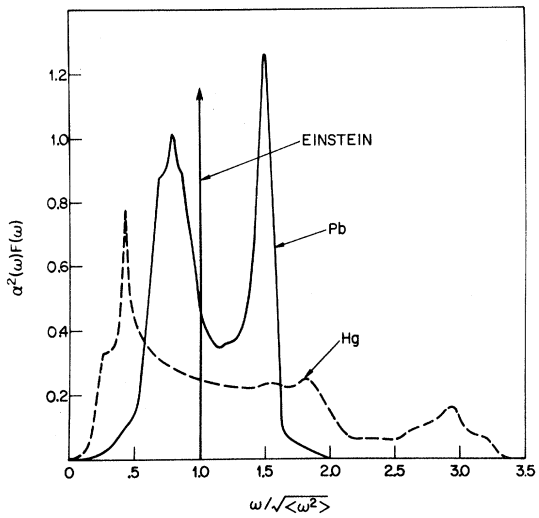

FIG. 5. Electron-phonon spectral functions $\alpha^2F(\omega)$ as measured by tunneling in Refs. 16 and 17. The frequency ω has been scaled to the rms frequency $(\langle\omega^2\rangle)^{1/2}$ in order to illustrate the relative deviations from the Einstein spectrum (also shown).

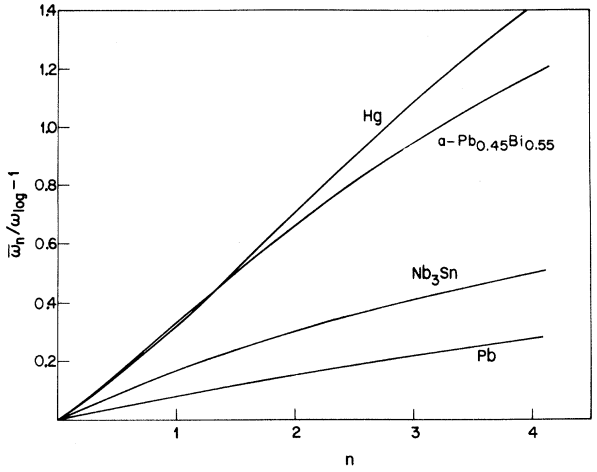

FIG. 7. Behavior of $(\langle\omega^n\rangle)^{1/n}\equiv\bar{\omega}_n$ as a function of n for various phonon distributions $\alpha^2F(\omega)$. In Appendix A it is proved that $\bar{\omega}_n$ is a nondecreasing function of n with the value ω_{log} in the limit $n\to 0$. An Einstein spectrum has $\bar{\omega}_n$ independent of n. The slope of the curves is a measure of the deviation from an Einstein spectrum, and the value $\bar{\omega}_2/\omega_{log}$ is a measure of the depression in $T_c/\bar{\omega}_2$ which results from the dispersion in $\alpha^2F(\omega)$. The curve labeled a-$Pb_{0.45}Bi_{0.55}$ is based on data from an amorphous film presented later in the paper.

with strong peaks at both 2 and 12 meV. In order to discuss the role of the shape of α^2F it is necessary to decide what parameters should remain invariant as the shape is altered. The natural choice is to fix λ and $\langle\omega^2\rangle$, which give the natural measures of the strength and the central frequency of α^2F, and also determine a unique T_c provided λ is very large. We are thus asking to know how T_c varies as the shape of α^2F varies with λ and $\langle\omega^2\rangle$ fixed. It has already been shown in Sec. II that

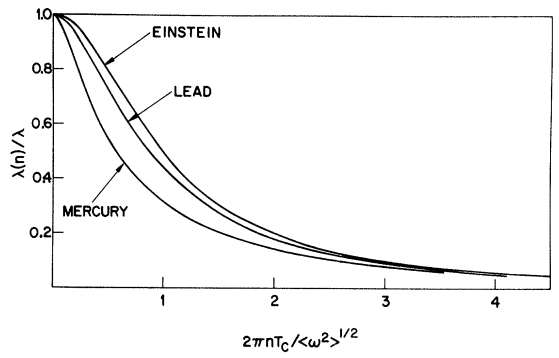

FIG. 6. Behavior of $\lambda(n)$ as defined in Eq. (4) normalized to λ plotted versus $x=2\pi nT_c/(\langle\omega^2\rangle)^{1/2}$. The effect of phonons on T_c is entirely contained in this function. At large x, this quantity behaves as $1/x^2$ for all phonon spectra. For an Einstein spectrum, the formula is $1/(1+x^2)$. In Appendix A it is shown that for an arbitrary phonon spectrum, $\lambda(n)/\lambda$ never exceeds the value it takes for an Einstein spectrum.

the maximum T_c under these conditions occurs for an Einstein spectrum.

We have made extensive solutions for T_c for the Einstein, lead, and mercury spectra. The shapes are shown in Fig. 5 with the frequency normalized to $(\langle\omega^2\rangle)^{1/2}$. For a strict comparison the strengths should have been normalized to unit λ, but lead and mercury have very similar values of λ, 1.55 and 1.6, respectively. The shape of α^2F enters the Eliashberg equations only via the ratio $\lambda(n)/\lambda$, where $\lambda(n)$ is defined in Eq. (10). The curves $\lambda(n)/\lambda$ versus n normalized to $n_0=(\langle\omega^2\rangle)^{1/2}/2\pi T_c$ are shown in Fig. 6. On this scale the Einstein spectrum is an upper bound for all n. This is proved in Appendix A and is the basis for the idea that the Einstein spectrum is optimal. For large values of n/n_0 the curves $\lambda(n)/\lambda$ all scale into $(n_0/n)^2$. This is the source of the shape independence of T_c at large λ.

Although the shape of α^2F enters most directly through the function $\lambda(n)/\lambda$, a more direct measure of the amount of dispersion of α^2F is obtained by comparing the various moments $\langle\omega^n\rangle$ or the average frequencies $\bar{\omega}_n$ [defined in Eq. (6)] for various values of n. The function $\bar{\omega}_n$ is plotted versus n in Fig. 7 for various metals, normalized to the limiting value as n goes to zero. It is shown in Appendix A that the limiting value can be written in the form

$$\omega_{log}\equiv\lim_{n\to 0}\bar{\omega}_n=\exp\left(\frac{2}{\lambda}\int_0^\infty\frac{d\omega}{\omega}\,\alpha^2F(\omega)\ln\omega\right). \qquad (30)$$

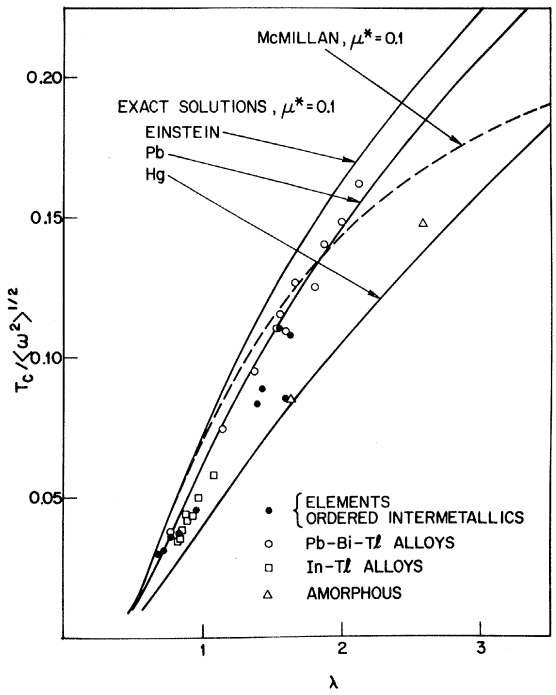

FIG. 8. $T_c/(\langle\omega^2\rangle)^{1/2}$ plotted versus λ. The solid curves are calculated for the various shapes of α^2F shown in Fig. 5 and with $\mu^*=0.1$. The dashed curve is the McMillan equation using $\mu^*=0.1$ and the prefactor $(\langle\omega^2\rangle)^{1/2}/1.20$ instead of $\theta_D/1.45$. The experimental points are taken from tunneling data given in Table I.

It is also shown in Appendix A that $\bar{\omega}_n$ is a nondecreasing function of n for $n>0$. As can be seen in Fig. 7, $\bar{\omega}_n$ tends to be roughly linear in n for small n, with mercury having a slope five times larger than lead. An Einstein spectrum is the only shape with zero slope.

To illustrate the effect of the shape of α^2F on T_c, Fig. 8 shows $T_c/\bar{\omega}_2$ plotted against λ. The theoretical calculations have been done for the three shapes of Fig. 5 and μ^* always 0.1. The experimental data are all taken from tunneling experiments and are tabulated in Table I. There is a surprisingly large sensitivity of $T_c/\bar{\omega}_2$ to the shape of the spectrum, especially considering that for $\lambda \gtrsim 10$, this sensitivity must disappear. The experimental points lie neatly between the extreme curves for Einstein and mercury spectra, and have a considerable amount of scatter. A small part of this scatter is a more or less random result of deviations of μ^* from 0.1, but the bulk of it is either a true shape effect or else experimental uncertainty. No single curve passes through the data well, and the McMillan equation fits the available data as well as any other curve on this graph.

An analysis of the McMillan equation by one of the authors[7] showed quite good agreement with experiment if the prefactor was chosen as $\langle\omega\rangle=\bar{\omega}_1$. Therefore, it is interesting to rescale the curves in Fig. 8 using $T_c/\bar{\omega}_1$ instead of $T_c/\bar{\omega}_2$. This is done in Fig. 9. There is now considerably less shape dependence in the three theoretical curves, and the data also show less scatter. The data have also been plotted this way in Ref. 16, except that the axes $(T_c,\ \lambda\bar{\omega}_1)$ were used instead of $(T_c/\bar{\omega}_1,\ \lambda)$ used here. The McMillan equation is noticably underestimating the trend in T_c for large λ. By inspection of Fig. 7, it is clear that if replacing $\bar{\omega}_2$ by $\bar{\omega}_1$ has eliminated some of the shape dependence, then replacing $\bar{\omega}_1$ by some $\bar{\omega}_n$ for $n<1$ will make even more improvement. This is confirmed in Fig. 10, where $T_c/\omega_{\log}$ is plotted versus λ. With this scaling, the shape dependence has been virtually eliminated for $\lambda<2$. The data are also quite satisfactorily aligned in this single curve, which deviates very noticeably from a McMillan curve at $\lambda=2$. The use of $\omega_{\log}$ as the appropriate scale factor has been proposed by Ginzburg and Kirzhnits[22,23] and is implicit in the work of Leavens.[24] Our calculations confirm this proposal for values $\lambda<2$. However, for large values of λ, the appropriate scaling frequency increasing from $\omega_{\log}$ to $\bar{\omega}_2$, the latter being appropriate for $\lambda>10$.

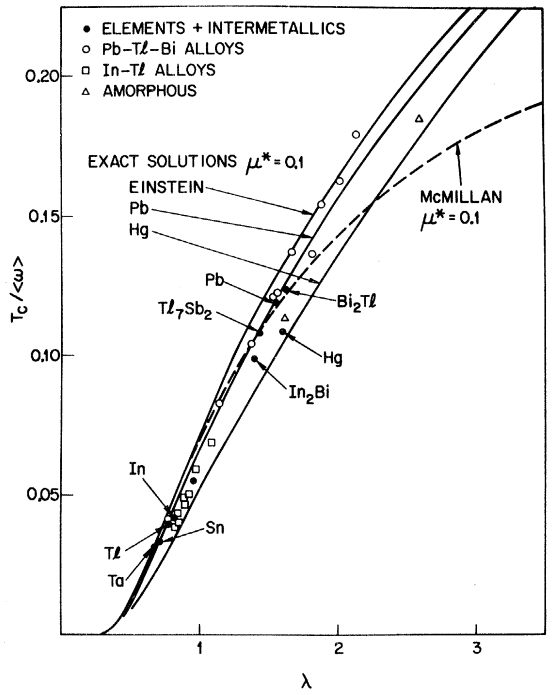

FIG. 9. $T_c/\langle\omega\rangle$ plotted versus λ. The solid curves and the data points are the same as in Fig. 8. The dashed curve is McMillan's equation with prefactor $\langle\omega\rangle/1.20$. Note that the scaling $T_c/\langle\omega\rangle$ is more successful than $T_c/(\langle\omega^2\rangle)^{1/2}$ in pulling the points and curves together towards a single curve.

TABLE I. Parameters[a] of superconductors derived from tunneling measurements. The value of μ^* is renormalized from previously reported values as described in the text.

Material	$\omega_{\log}$ (K)	$\overline{\omega}_1$ (K)	$\overline{\omega}_2$ (K)	λ	ω_{ph} (K)	$\mu^*(\omega_{ph})$	T_c (K)	η (eV/Å^2)
Pb	56	60	65	1.55	110	0.105	7.2	2.4
In	68	79	89	0.805	179	0.097	3.40	1.3
Sn	99	110	121	0.72	209	0.092	3.75	2.2
Hg	29	38	49	1.6	162	0.098	4.19	1.4
Tl	52	58	64	0.795	127	0.111	2.36	1.2
Ta	132	140	148	0.69	228	0.093	4.48	4.9
a-Ga	55	77	101	1.62	291	0.095	8.56	2.1
β-Ga	87	108	129	0.97	285	0.092	5.90	2.0
$Tl_{0.9}Bi_{0.1}$	48	55	62	0.78	120	0.099	2.30	1.1
$Pb_{0.4}Tl_{0.6}$	48	56	62	1.15	121	0.094	4.60	1.6
$Pb_{0.6}Tl_{0.4}$	50	57	62	1.38	119	0.103	5.90	2.0
$Pb_{0.8}Tl_{0.2}$	50	56	61	1.53	116	0.101	6.80	2.1
$Pb_{0.6}Tl_{0.2}Bi_{0.2}$	48	53	58	1.81	112	0.111	7.26	2.3
$Pb_{0.9}Bi_{0.1}$	50	56	60	1.66	108	0.081	7.65	2.2
$Pb_{0.8}Bi_{0.2}$	46	52	57	1.88	109	0.093	7.95	2.3
$Pb_{0.7}Bi_{0.3}$	47	52	57	2.01	110	0.092	8.45	2.4
$Pb_{0.65}Bi_{0.35}$	45	50	55	2.13	110	0.093	8.95	2.4
$In_{0.9}Tl_{0.1}$	63	75	86	0.85	176	0.103	3.28	1.4
$In_{0.73}Tl_{0.27}$	55	67	77	0.93	166	0.110	3.36	1.4
$In_{0.67}Tl_{0.33}$	57	68	79	0.90	167	0.110	3.26	1.4
$In_{0.57}Tl_{0.43}$	53	64	74	0.85	165	0.117	2.60	1.3
$In_{0.5}Tl_{0.5}$	53	64	73	0.83	163	0.110	2.52	1.3
$In_{0.27}Tl_{0.73}$	42	53	63	1.09	151	0.094	3.64	1.4
$In_{0.17}Tl_{0.83}$	45	55	63	0.98	144	0.101	3.19	1.3
$In_{0.07}Tl_{0.93}$	49	56	63	0.89	131	0.107	2.77	1.3
In_2Bi	46	57	67	1.40	174	0.096	5.6	1.6
Sb_2Tl_7	37	48	58	1.43	134	0.102	5.2	1.6
Bi_2Tl	47	53	59	1.63	120	0.101	6.4	2.1
a-$Pb_{0.45}Bi_{0.55}$	29	38	47	2.59	128	0.116	7.0	2.1

[a]Tabulation of the data used to derive these parameters is available in J. M. Rowell, W. L. McMillan, and R. C. Dynes, J. Phys. Chem. Ref. Data (to be published).

IV. TUNNELING DATA

The data with which we compare our calculations is that obtained from superconducting tunneling measurements. Via quasiparticle tunneling through thin insulating barriers in the configuration normal-metal–insulator–superconductor, and normalizing this with measurements when the superconductor is in the normal state, direct information about the density of quasiparticle excitations and hence the function $\alpha^2F(\omega)$ can be obtained. From the ratio of conductances in the superconducting, $\sigma_S(\omega)$, and normal $\sigma_N(\omega)$ states, one obtains

$$\frac{\sigma_S(\omega)}{\sigma_N(\omega)} = \frac{N_S(\omega)}{N_N(\omega)} = \mathrm{Re}\left(\frac{\omega}{[\omega^2 - \Delta^2(\omega)]^{1/2}}\right). \tag{31}$$

Here $N_{S\,(N)}$ is the density of excitations in the superconducting (normal) state and $\Delta(\omega)$ is the complex energy-dependent energy-gap parameter which reflects the strong electron-phonon coupling in its detailed structure. Using an iterative unfolding procedure the gap parameter $\Delta(\omega)$ and the spectral function $\alpha^2F(\omega)$ are extracted from the conductance data by inversion of the zero-temperature Eliashberg gap equations.

The zero-frequency energy gap Δ_0 is also directly measured in a tunneling experiment. This parameter is a direct measure of the net attractive interaction a pair experiences, i.e., the sum of the attractive part [as represented by $\alpha^2F(\omega)$, or more properly λ] and the Coulomb repulsion $-\mu^*$. Hence we have, in addition to $\alpha^2F(\omega)$, a measure of μ^*. We saw in the preceding sections that this term depends on one's choice of cutoff energies for the electrons and phonons of the system. In practice, in the solution of the Eliashberg gap equations to extract $\alpha^2F(\omega)$, the integrations are performed to a cutoff frequency ω_{co}, which is ≈ 10 ω_{ph}, where ω_{ph} is the cutoff energy of the phonon spectrum. Beyond $10\omega_{ph}$, $\Delta(\omega)$ is structureless and hence further integration is unnecessary. The actual value of μ^* used in the inversion process to fit Δ_0 is scaled to this (arbitrarily chosen) frequency ω_{co}. It has been the usual practice to publish

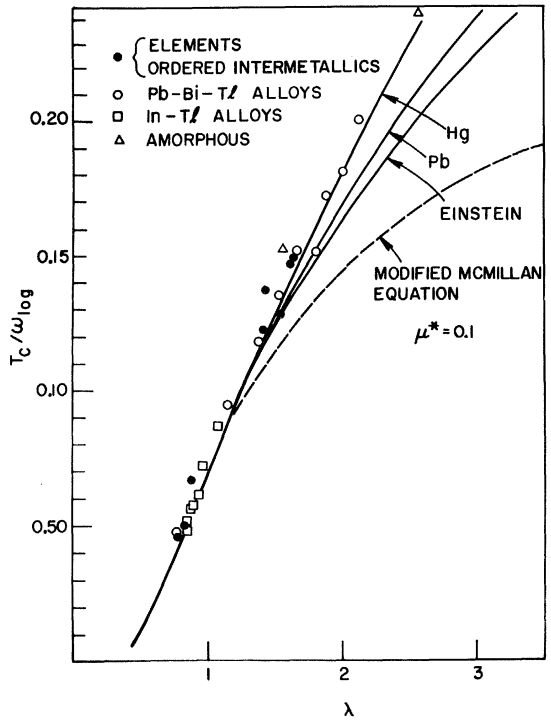

FIG. 10. T_c/ω_{log} plotted versus λ. The solid curves and the data points are the same as in Fig. 8. The dashed curve is McMillan's equation with prefactor $\omega_{log}/1.20$. Note that the scaling T_c/ω_{log} has produced a universal curve describing all the experiments and calculations for $\lambda<1.5$.

as the "experimental" value, the parameter $\mu^*(\omega_{co})$ used in the computer program, rather than the more physical parameter defined in Eqs. (4) and (12),

$$\frac{1}{\mu^*(\omega_{ph})}=\frac{1}{\mu^*(\omega_{co})}+\ln\left(\frac{\omega_{co}}{\omega_{ph}}\right). \tag{32}$$

The values of $\mu^*(\omega_{ph})$ shown in Table I are defined by Eq. (32). This convention is more "physical" in being more closely related to an approximate T_c equation, and also eliminates the arbitrary dependence of μ^* on the choice of cutoff in the solution of the gap equations. We recommend that experimental values of μ^* be presented in this fashion in the future to avoid ambiguities and make the values consistent with those deduced from the isotope effect. In most cases, the differences are small and do not affect calculations or results. However, when one is testing consistency, as is done here, the differences become important and must be accounted for. This has also been noticed by Leavens.[19]

In Table I we compile the results of tunneling measurements on the materials where all this information is available. We present the various moments (ω_{log}, $\bar{\omega}_1$, $\bar{\omega}_2$) of the function $\alpha^2F(\omega)$ which are used in these calculations, λ, the experimentally measured T_c, the renormalized $\mu^*(\omega_{ph})$, and the parameter η, which is obtained from the relationship

$$\lambda=\frac{N_t(0)\langle I^2\rangle}{M\langle\omega^2\rangle}=\frac{\eta}{M\langle\omega^2\rangle}. \tag{33}$$

Here $\langle I^2\rangle$ is the average over the Fermi surface of the electron-phonon matrix element and M is the atomic mass. The importance of this parameter and speculations concerning it will be presented in Sec. VI.

We see from this compilation that except for Ta, the materials for which data are available are all s-p or "soft" materials. This is for a purely practical reason as the d- and f-band materials are more difficult to prepare pure and the results are more sensitive to any impurities on the surfaces because of the relatively short coherence lengths. It is also clear from this table that the values of λ obtained to date are $\lesssim 2$. This explains why the McMillan equation has done quite well in describing these systems except for the few materials with $\lambda>1.5$. It is clear, however, from Fig. 10, that for $\lambda>2$, substantial deviations from the McMillan equation are predicted from our calculations and indicated by the strong-coupled Pb-Bi alloys.

In an attempt to obtain a value of λ greater than found in crystalline alloys we have followed previous investigators and prepared an amorphous Pb-Bi alloy. The concentration chosen was $Pb_{0.45}Bi_{0.55}$ and the alloy was evaporated from a resistively heated boat onto a substrate held close to 4.2 K. The tunnel-junction configuration was of the type Al-oxide-amorphous film and the tunneling measurements were preformed at 1.05 K for the superconducting state and 8.0 K for the normal state. Care was taken to measure the conductances to as low an energy (or voltage) as was possible, to reduce the influence of assumptions on the functional form of $\alpha^2F(\omega)$ at low ω. Below a certain energy it becomes difficult to measure accurately the conductance and an ω^2 dependence to $\alpha^2F(\omega)$ has traditionally been assumed. This assumption has been criticized especially in the amorphous materials, where because there is a large density of states at low ω the assumption becomes more critical than in crystalline systems. The parameters λ and $\bar{\omega}_n$ depend *critically* on these choices. The surest way to avoid these problems is to measure to as low an energy as possible, and hence the $\alpha^2F(\omega)$ is "measured," not assumed. It is for these reasons (as well as the inaccessibility of the parameter ω_{log}) that we choose not to include in Table I previous measurements of amorphous materials similar to those reported here. The measurements were thus made down to 0.25 meV above the

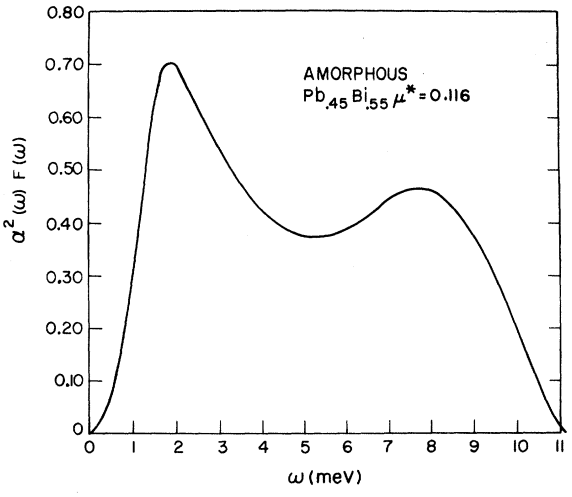

FIG. 11. $\alpha^2F(\omega)$ versus ω for the amorphous alloy $Pb_{0.45}Bi_{0.55}$. The material was quench condensed on a substrate held close to 4.2 K.

gap and the resultant $\alpha^2F(\omega)$ is shown in Fig. 11. It is clear from this figure that the shape and strength do not significantly depend on a functional choice below 0.25 meV as there is very little weight below here. The various moments as well as λ, μ^*, and the measured T_c are included at the end of Table I, where we see that the value for λ is 2.59, higher than for any known crystalline system. The value of $T_c/\omega_{\log}$ is 0.284 and on the plot of $T_c/\omega_{\log}$ vs λ of Fig. 10, is shown as the triangle at the extreme end. This provides a very clear illustration in the strong-coupling limit that McMillan's equation breaks down and a modified form for the dependence of T_c on these parameters is needed. We choose to modify McMillan's equation rather than propose anything radically different and in Sec. V we suggest these modifications.

V. APPROXIMATE T_c EQUATION

Many authors have proposed approximate equations relating T_c to μ^* and various integrals over α^2F such as λ, ω_1, ω_2, etc. Of these equations, McMillan's form,[1] Eq. (2), is the best known and most useful by virtue of priority, simplicity, relative accuracy, and wealth of documentation. Therefore we do not propose to abondon McMillan's equation, but rather to provide some correction factors which have the value unity for most known materials and extend and range of McMillan's equation to cover extreme cases.

McMillan's formula is based on 22 numerical solutions of the Eliashberg equations for $0 \leq \mu^* < 0.25$ and $0 < \lambda < 1.5$, using a single shape for α^2F patterned after the phonon density of states of Nb. We have performed more than 300 numerical solutions of the Eliashberg equations for a number of shapes, and values of λ up to 10^6. Of these we have selected for purposes of fitting 217 calculations representing the range $0 \leq \mu^* \leq 0.20$, $0.3 < \lambda < 10$, and three shapes (Pb, Hg, and Einstein). Representative results are shown in Fig. 12. The correction factors to McMillan's equation must account for both the shape dependence and the enhanced values of T_c as the asymptotic regime $T_c \sim \lambda^{1/2}$ is approached.

As discussed in Sec. III, the shape dependence of T_c is eliminated for $\lambda < 2$ if the prefactor of McMillan's equation is changed from ω_1 to $\omega_{\log}$. With this single correction, the McMillan equation becomes highly accurate for all superconductors with $\lambda \lesssim 1.5$. We have not increased the number of parameters (λ, μ^*, $\omega_{\log}$) necessary to describe T_c. For empirical purposes, one would prefer instead of $\omega_{\log}$ a prefactor that was accessible by some experiment simpler than tunneling. The most obvious such parameter is Θ_D, as BCS and McMillan suggested, but unfortunately this is not very accurate. A systematic search for an accurate and accessible characteristic temperature has not been made but would be of considerable value. For simple materials (i.e., elements), where α^2F is roughly proportional to F, $\omega_{\log}$ could be estimated from heat-capacity or neutron scattering data. For complicated materials little data exist, but there is no firm reason for α^2F to remain proportional to F.

It can be seen from Fig. 10 that $T_c/\omega_{\log}$ starts to become shape dependent for $\lambda \gtrsim 1.6$. This is somewhat larger than the value of λ ($\gtrsim 1.3$), where strong-coupling corrections (characterized by the enhancement of the solid curves relative to the dashed McMillan curve) begin to appear. Therefore we use two separate correction factors (f_1 and

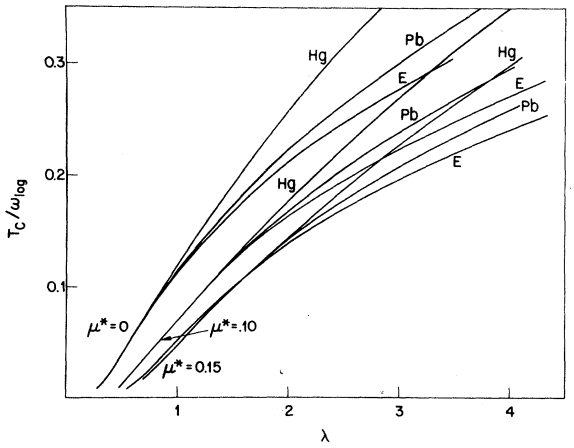

FIG. 12. $T_c/\omega_{\log}$ versus λ for three shapes of α^2F and three values of μ^*. This figure summarizes about 50% of the numerical calculations used in constructing the corrections to McMillan's equation.

TABLE II. "Empirical" values of λ for some bcc transition metals and Nb_3Sn. The empirical values of ω_{log}, ω_1, ω_2 are calculated from Born–von Karman analysis of neutron data assuming $\alpha^2F=F$, or (where indicated) from tunneling measurements of α^2F. The values of λ found by McMillan (column 8) were calculated assuming $\mu^*=0.13$ and taking $\Theta_D/1.45$ as the prefactor in the McMillan equation. We find the prefactor $\omega_{log}/1.2$ is smaller than $\Theta_D/1.45$ and consequently obtain larger values of λ (column 7). However, if μ^* is assumed to be 0.1 (arguments in favor of this are given in the text), then values of λ very similar to McMillan's are found (column 6). In the case of Nb_3Sn, the tunneling experiment doesn't yield an accurate experimental value of λ; our calculated values of λ can be used to normalize the experimentally measured $\alpha^2F(\omega)$. Values of η (column 11) are calculated using λ from column 6 and $\langle\omega^2\rangle$ from column 5. These differ from McMillan's values of η because of a difference in $\langle\omega^2\rangle$, and are in better agreement with the theory of Evans *et al.* (Ref. 30).

Material	$\bar{\omega}_{log}$(K)	$\bar{\omega}_1$(K)	$\bar{\omega}_2$(K)	T_c(K)	λ Eq. (34) $\mu^*=0.10$	λ Eq. (34) $\mu^*=0.13$	λ McMillan Ref. 1 $\mu^*=0.13$	λ (expt)	μ^* (expt)	η (eV/Å^2)
1	2	3	4	5	6	7	8	9	10	11
V	222	230	238	5.30	0.60	0.67	0.60	···	···	3.1
Cr	308	317	324	···	···	···	···	···	···	···
Nb	166	175	183	9.22	0.85	0.94	0.82	···	···	4.7
Mo	236	244	251	0.92	0.39	0.45	0.41	···	···	4.2
Ta	142	148	153	4.48	0.67	0.74	0.65	···	···	5.1
Ta (tunneling)	132	140	148	4.48	0.69	0.76	0.65	0.69	0.093	4.9
W	208	215	220	0.012	0.25	0.28	0.28	···	···	4.5
Nb_3Sn (tunneling)	125	146	163	18.1	1.67	1.83	···	···	···	7.9

f_2) to describe these two effects:

$$T_c=\frac{f_1f_2\omega_{log}}{1.20}\exp\left(-\frac{1.04(1+\lambda)}{\lambda-\mu^*-0.62\lambda\mu^*}\right). \quad (34)$$

We have found approximate formulas for f_1 and f_2 which involve only one additional parameter, $\bar{\omega}_2=\langle\omega^2\rangle^{1/2}$. By requiring f_1 and f_2 to be unity for small λ we ensure a good fit at small λ. The "strong-coupling correction" f_1 must scale as $\lambda^{1/2}$ for large λ, while the "shape correction" f_2 must go to $\bar{\omega}_2/\omega_{log}$ at large λ. Acting together, these two corrections allow Eq. (34) to attain the correct asymptotic behavior given in Eq. (22). We have somewhat arbitrarily chosen the forms

$$f_1=[1+(\lambda/\Lambda_1)^{3/2}]^{1/3}, \quad (35)$$

$$f_2=1+\frac{(\bar{\omega}_2/\omega_{log}-1)\lambda^2}{\lambda^2+\Lambda_2^2}. \quad (36)$$

The exponents in these equations could have been altered somewhat; our choice represents a compromise between simplicity and accuracy. The parameters Λ_1 and Λ_2 are given by

$$\Lambda_1=2.46(1+3.8\mu^*), \quad (37)$$

$$\Lambda_2=1.82(1+6.3\mu^*)(\bar{\omega}_2/\omega_{log}), \quad (38)$$

where the numerical coefficients have been chosen by least-squares analysis of the 217 selected numerical solutions. The rms percent deviation is 5.6%.

One of the principal uses of approximate T_c equations is the estimation of approximate "empirical" values of λ from measured values of T_c. We illustrate this in Table II, where new empirical values of λ are obtained for five bcc transition elements. Because the values of λ are all below 1, the correction factors f_1 and f_2 are entirely negligible. There are two sources of uncertainty in the empirical values of λ. The largest source is the value of ω_{log}. This uncertainty accounts for disagreements of greater than 10% between our estimates of λ and McMillan's for some materials. McMillan used values of $\Theta_D/1.45$ while we have used $\bar{\omega}_{log}/1.2$, where $\bar{\omega}_{log}$ is computed from the phonon density of states $F(\omega)$ in the same way that ω_{log} is computed from $\alpha^2F(\omega)$. The similarity[6] between $\alpha^2F(\omega)$ as measured by tunneling[25] and $F(\omega)$ as deduced from neutron scattering in tantalum suggests that $\bar{\omega}_{log}$ should be an excellent approximation to ω_{log} in these materials. A second source of uncertainty is empirical values of λ is the uncertainty in μ^*. We do not follow McMillan in assuming $\mu^*=0.13$ for all transition elements. For the bcc transition elements, the isotope effect in Mo and tunneling in Ta yield values of μ^* of 0.09. McMillan suggested that a larger value of μ^* should occur for transition metals than for s-p metals because of a larger μ [both $N(0)$ and V_c are probably larger] and a smaller $\ln(\omega_{el}/\omega_{ph})$. Garland[26] also suggested that $\ln(\omega_{el}/\omega_{ph})$ was smaller in transition elements in order to explain isotope effects. However, we suggest that the latter factor probably increases rather than decreases for transition elements. The electronic cutoff ω_{el} is defined by the cutoff in $\mathrm{Im}[1/\epsilon(Q,\omega)]$, just as ω_{ph} is the cutoff of $\alpha^2F(\omega)$. Recent optical measurements[27] show that $\mathrm{Im}[1/\epsilon(0,\omega)]$

remains large at energies of 30 eV and more in Nb and Mo. There may be an order-of-magnitude increase in ω_{el} or a factor of 4 increase in ω_{el}/ω_{ph}, which is enough to compensate a factor of 3 increase in μ above the value ~ 0.5 characteristic of nontransition metals. Thus we have taken $\mu^* = 0.10$ for all metals. Isotope-effect and tunneling measurements suggest a fairly large variation in μ^* about this figure, but it is not clear how reliable these "measurements" of μ^* really are.

It should be clear from the examples in Table II that a fairly large uncertainty should be attached to the empirical values of λ owing to uncertainty in ω_{log} and μ^*. The uncertainty is larger for compounds than for elements because ω_{log} is more uncertain. Very little information exists as to how the optic phonons should be weighted in ω_{log}.

VI. HIGH T_c: CAUSES AND LIMITATIONS

Before McMillan's work[1] there was virtually no theoretical understanding of the causes of or limitations to high T_c's. McMillan observed that the column-V transition metals (V, Nb, Ta) had values of λ roughly twice as large as the values found in the neighboring column-VI elements (Cr, Mo, W), and that this increase could be explained as coming entirely from the softening of the rms phonon frequency $(\langle\omega^2\rangle)^{1/2}$. He found a rigorous relation between λ and $\langle\omega^2\rangle$, given in Eq. (33). The numerator of (33), η, is a purely electronic property, independent of lattice dynamics. Hopfield[28] showed how η can be regarded as a local "chemical" property of an atom in a crystal, and Gaspari and Gyorffy[29,30] discovered a simple way of calculating η in a muffin-tin approximation if the electron scattering phase shifts of a crystal potential are known. The principle ingredient lacking is a theoretical understanding of the parameter $\langle\omega^2\rangle$, and a number of groups are gradually providing answers to that problem.[31,32]

However, in spite of these important achievements, theory has yet to provide concrete help in understanding high-T_c materials or raising T_c. Our analysis of theory and experiment finds that the situation has been muddied by several misconceptions which we here attempt to straighten out. These misconceptions are as follows: the importance of softening phonons (i.e., $\langle\omega^2\rangle$) and the "$\lambda = 2$ limit." Both of these arose in McMillan's work from the extrapolation of observations which seem entirely correct for materials with $\lambda < 1$ into the (then unexplored) regime with $\lambda > 1$. McMillan made suitable cautionary and qualifying remarks which have been largely forgotten with time.

A related question (which McMillan did not consider) is how should $\alpha^2F(\omega)$ be changed to get the maximum benefit to T_c. This question was given an elegant answer by Bergmann and Rainer,[10] who calculated the functional derivative $\delta T_c/\delta\alpha^2F(\omega)$, which is defined by

$$\Delta T_c = \int_0^\infty d\omega \, \frac{\delta T_c}{\delta\alpha^2F(\omega)} \, \Delta\alpha^2F(\omega) \, . \tag{39}$$

The results of Ref. 10 show that increasing $\alpha^2F(\omega)$ at *any* value of ω *always* increases T_c (in contradiction to the incorrect conclusion of Ref. 12 that coupling to very-low-frequency phonons could decrease T_c). Furthermore, there is a frequency range near $\omega = 2\pi T_c$ where T_c is most favorably enhanced by an increase of $\alpha^2F(\omega)$. Following the method of Ref. 10, we have calculated $\delta T_c/\delta\alpha^2F(\omega)$ for the lead spectrum. Results are shown in Fig. 13 for various assumed magnitudes of T_c. For actual Pb with $T_c/(\langle\omega^2\rangle)^{1/2} \sim 0.1$, the optimum frequency occurs in the region of the TA phonons. For higher-T_c materials, the magnitude of the functional derivative falls, indicating that it is increasingly difficult to raise T_c (i.e., the slope of T_c versus λ is decreasing as λ increases). The benefit of robbing from α^2F at high ω to increase it at low ω becomes increasingly small as T_c gets higher.

Based on his observations on the column-V and -VI bcc transition elements, McMillan proposed that the best hope for raising λ and T_c was by decreasing $\langle\omega^2\rangle$, since η appeared to be roughly invariant in a given class of materials. There is now good experimental evidence[28] pointing to the opposite conclusion, namely, that *for strong-coupling*

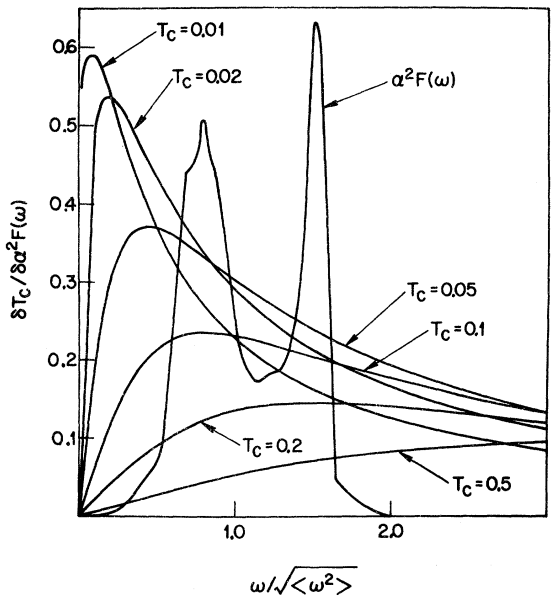

FIG. 13. Functional derivative $\delta T_c/\delta\alpha^2F(\omega)$ plotted versus $\omega/(\langle\omega^2\rangle)^{1/2}$, for six different assumed values of $T_c/(\langle\omega^2\rangle)^{1/2}$. The calculations were done for $\mu^* = 0.1$. The shape of $\alpha^2F(\omega)$ is that of lead and is shown (with unspecified amplitude) for purposes of comparison.

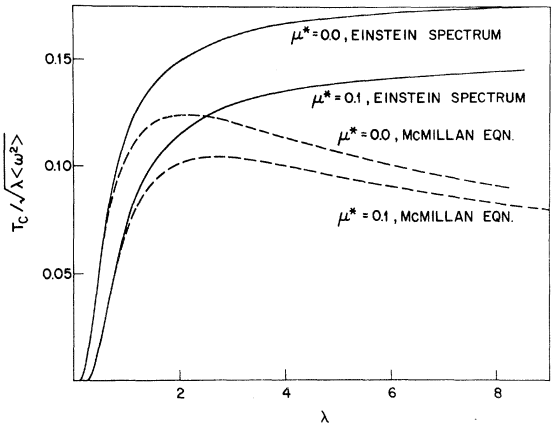

FIG. 14. Variation of T_c with λ keeping $\lambda\langle\omega^2\rangle$ fixed. Exact solutions of Eq. (14) with an Einstein spectrum (solid curves) are compared with the results from McMillan's Eq. (2) (dashed curves) for $\mu^*=0$ and $\mu^*=0.1$. The value of T_c is normalized to the constant $(\lambda\langle\omega^2\rangle)^{1/2}$. The maxima at $\lambda=2$ and $\lambda=2.6$ found from McMillan's equation with $\mu^*=0.1$ are spurious. The true maxima are at $\lambda=\infty$.

systems, variation in η is more important than variation of $\langle\omega^2\rangle$ in causing T_c to change. Softening of $\langle\omega^2\rangle$ often does enhance T_c, but very high T_c seems to be caused more by large η than by small $\langle\omega^2\rangle$. McMillan also showed that if η/M or $\lambda\langle\omega^2\rangle$ was invariant in a system (this now appears to be the exception rather than the rule), then according to the McMillan equation there is an optimum value of λ (near 2) and a maximum value of T_c. This is illustrated in Fig. 14, where theoretical values of T_c normalized to $(\lambda\langle\omega^2\rangle)^{1/2}$ are plotted *versus* λ. For $\mu^*=0.1$, McMillan's equation has a broad maximum, $T_c\sim 0.105\,(\lambda\langle\omega^2\rangle)^{1/2}$, occurring at $\lambda=2.6$. However, *this result is spurious*, being based on an extrapolation that fails for $\lambda>1$. The true solutions of the Eliashberg equations are monotonically increasing with λ, even if $\lambda\langle\omega^2\rangle$ is held fixed. The actual maximum is $T_c\sim 0.15\times(\lambda\langle\omega^2\rangle)^{1/2}$ (assuming $\mu^*=0.1$), occurring when $\lambda>10$. Thus McMillan has underestimated the maximum value of $T_c/(\lambda\langle\omega^2\rangle)^{1/2}$ by about 40%, underestimated the virtue of having λ much greater than 1, and underestimated the degree to which the "chemical" parameter η can be varied. All these reconsiderations are optimistic for high T_c's, and we need now to examine what prevents real materials from attaining the high T_c's which Eliashberg theory seems to allow.

We first analyze a system that seems to obey the $\lambda=2$ limit, namely, Pb and some isoelectronic analogs. With $\lambda=1.55$, Pb lies close to the $\lambda=2$ limit and has T_c within 4% of the maximum (if the more realistic curve for $\mu^*=0.1$ is used in Fig. 13, then the optimum λ is 2.6 and T_c for Pb is 12% short of the maximum). If the McMillan equations were correct *and* if η were invariant, then there would be little hope for increasing T_c in Pb. Surprisingly, the data of Table III seem to support this. Both the disordered crystalline ternary $Pb_{0.6}Tl_{0.2}Bi_{0.2}$ and amorphous Pb films have the same values of T_c as crystalline Pb, although λ is enhanced in the disordered systems. Closer inspection shows that the reason T_c is not enhanced has nothing to do with the $\lambda=2$ limit, but rather occurs because η has decreased (for reasons not entirely clear).

A different and more interesting behavior occurs in Pb if the electron concentration ($\mathfrak{z}$) is increased by alloying with Bi. Tunneling data for this system are reported by Dynes and Rowell[33] and are included in Table I. In these alloys T_c rises monotonically with $\mathfrak{z}$ to a maximum of 8.95 K at $Pb_{0.65}Bi_{0.35}$. Beyond this concentration Bi is no longer soluble in Pb. With no data available at the time, McMillan suggested that the limiting T_c might occur because $\langle\omega^2\rangle$ had decreased to a point of lattice instability. However, neither tunneling[33] nor neutron scatterint[34] data suggest a significant decrease in $\langle\omega^2\rangle$ or a dangerously soft mode in this system. A more plausible interpretation[35] is that the first-order instability at 4.35 electrons/atom ($\mathfrak{z}$) is a "covalent instability" occurring because a large s-p electron concentration favors directional covalent bonding as occurs in Bi. The increase in T_c from 7.2 to 8.95 K occurs primarily through an increase in η from 2.3 at $\mathfrak{z}=4$ ($Pb_{0.6}Tl_{0.2}Bi_{0.2}$) to 2.4 at $\mathfrak{z}=4.35$. (These values of η are calculated for disordered crystalline alloys; ordered Pb with $\eta=2.4$ deviates by +0.2 from a smooth curve drawn for η versus $\mathfrak{z}$ in the disordered Tl-Pb-Bi system.) The data tend to suggest that as η increases, so does the ability to form covalent bonds, leading to an upper limit of 2.4 on η in this system, at which point a transition occurs to a more covalent nonmetallic structure.

Further confirmation of the nonconstancy of η was given by Weber,[36] who studied the lattice dynamics of Nb-Mo alloys. McMillan found that pure

TABLE III. Illustrating the (unexplained) futility of increasing T_c in a strong-coupling system by decreasing $\langle\omega^2\rangle$. McMillan's explanation of the futility was the (spurious) "$\lambda=2$ limit." The tunneling experiments have now shown that η was reduced (this is the unexplained feature) rather than remaining constant is expected.

	$(\langle\omega^2\rangle)^{1/2}$ (K)	λ	$\lambda M\langle\omega^2\rangle=\eta$ (eV/Å^2)	T_c
Pb	64	1.55	2.4	7.20
$Pb_{0.6}Tl_{0.2}Bi_{0.2}$	58	1.81	2.3	7.26
a-Pb	53	1.91	2.0	7.2
a-$Pb_{0.45}Bi_{0.55}$	47	2.59	2.1	7.0

TABLE IV. Illustrating the origin of strong electron-phonon coupling and large values of T_c. The reason for higher T_c's in d-band materials than in s-p-band materials is the larger value of $\omega_{\log}$. The difference between the medium- and strong-coupling materials is a factor of 2 increase in λ *arising primarily* from an increase in η, rather than a decrease in $\langle\omega^2\rangle$. In all these examples, $\langle\omega^2\rangle$ is anomalously low (compare Pb and Tl with Au, or Nb, and Nb_3Sn with Mo). A decrease of $\langle\omega^2\rangle$ does account for a factor of 2 increase in λ between Mo and Nb, but this factor seems to play a much smaller role in high-T_c materials. The data are all from Table I or II.

	Medium coupling	Strong coupling
	Tl	Pb
s-p metals	$T_c = 2.4$ K	$T_c = 7.2$ K
	$\lambda = 0.795$	$\lambda = 1.55$
$M \approx 200$ amu	$\omega_{\log} = 52$ K	$\omega_{\log} = 56$ K
	$\eta = 1.2$ eV/Å^2	$\eta = 2.4$ eV/Å^2
	Nb	Nb_3Sn
d metals	$T_c = 9.2$ K	$T_c = 18.1$ K
	$\lambda = 0.85$	$\lambda = 1.67$
$M \approx 100$ amu	$\omega_{\log} = 166$ K	$\omega_{\log} = 125$ K
	$\eta = 4.7$ eV/Å^2	$\eta = 7.9$ eV/Å^2

Nb and Mo have values of λ differing by a factor of 2, while η differs by less than 10%. However, Weber found significant variations of η (up to 40%) in Nb-Mo alloys, the variations correlating with the variation of λ and T_c. Thus it is now certain that the factors which govern the value of η are not simply crystal structure and electron type as speculated by McMillan, but also electron concentration and crystalline order. Even the density of states $N(0)$ still plays a role, although somewhat canceling as Hopfield[28] showed for d-band materials.

Our own point of view on the nature of high-T_c materials is illustrated by the 4 materials shown in Table IV, with T_c ranging from 2 to 18 K. Our aim is simply to identify which material property makes T_c higher in one material than in another. We feel this provides a necessary ingredient (a usable recipe is still lacking) for raising T_c. The first two materials, Tl and Pb, represent a medium-coupling and a strong-coupling s-p material. The increase in T_c from 2.4 to 7.2 K is emphatically not coming from softening of phonons. Both materials have low phonon frequencies (a factor of 2.3 in $M\omega^2$ softening has occurred relative to Au). The increase in T_c arises from a factor of 2 increase in η which causes a factor of 2 increase in λ. The value $\eta = 2.4$ may represent the maximum that a material based on Pb can sustain because of the covalent instability. As prototype examples of covalent instability, we take the first row of the Periodic Table. The potential for high T_c's in these materials is evident in the value $T_c = 9.6$ K found in amorphous Be films,[37] and in the predicted high T_c's for metallic hydrogen.[38] Crystalline Be has $T_c \sim 0.3$ K and $\lambda \sim 0.23$. The value of η is quite uncertain because of uncertainty in $\langle\omega^2\rangle$; based on $\Theta_D = 1390$ K we estimate $(\langle\omega^2\rangle)^{1/2} \sim 800$ K, which gives $\eta = 2.4$. The large T_c in amorphous films could be explained in both λ and η had doubled with $\langle\omega^2\rangle$ unchanged. This gives a value $\eta \sim 5$, which is very large for an s-p material and suggests that crystalline Be has a reduced T_c because of a covalent instability. There are in fact solid reasons for regarding the low T_c of Be as arising from a low $N(0)$ (about one-third as large as an equal density electron gas). The low $N(0)$ is a result of having an even number of electrons in the unit cell and a strongly contracted Fermi surface because of wide covalent[39] gaps at the zone boundary. Beryllium almost succeeds in becoming a semiconductor like its neighbor, boron.

To summarize for s-p metals, they do not have high T_c's primarily because the phonon energy $\omega_{\log}$ is too low. The maximum T_c appears to be limited by a covalent instability occurring when η is too large. The largest η may occur in amorphous Be, but there $\langle\omega^2\rangle$ is large and λ is low. To raise T_c one needs to have both λ and $\omega_{\log}$ large, and this requires large η. Large η means strong electron-ion interaction.

In transition elements, larger values of η occur because the d wave functions are contracted towards the core and have a strong electron-ion interaction. Because of the attraction to the core, they are also less subject to covalent instabilities. However, if the wave function is too much contracted, the resulting narrow bands have magnetic instabilities which prevent superconductivity (as in $3d$- or f-band metals). From Table IV we see that Nb has a value of η twice as large as Pb, but T_c is only slightly larger. The trouble is that $M\langle\omega^2\rangle$ has increased by almost a factor of 4 so that λ has decreased by 2. This is offset by a factor of 3 improvement in $\omega_{\log}$. It appears very hard to adjust the parameters of a transition metal to get λ large because of the stiff lattices and the apparent difficulty of getting $\eta > 5$.

What then is the nature of the known high-T_c materials? Table IV shows our estimates of the parameters of Nb_3Sn, the best known of high-T_c materials. The striking feature is that λ has increased by a factor of 2 over Nb *without* sacrificing too much of $\omega_{\log}$. This can only happen by a still further increase in η. The source of this increase in η is not clear, but the $A15$ crystal structure must play an important role. The structure is cubic, but the Nb atoms are on sites of low point symmetry, with only two first neighbors which make the anomalously close-packed chains. This close-neighbor distance and low coordination number is an indicator of covalency, and may invalidate

the muffin-tin assumption which lies beneath Hopfield's analysis of η. It is tempting to speculate that the large η arises from the breakdown of muffin-tin analysis. Another crystal structure with anomalously close neighbor distances is the AlB_2 structure, which exhibits among the highest T_c's of any hexagonal metals.[40] It is also interesting to note that Hopfield's work[28] indicates that large η requires the simultaneous presence at the Fermi surfaces of electrons of two different partial-wave symmetries satisfying $\Delta l = \pm 1$. This requirement is also clearly beneficial to covalent-bond formation, as directional bonding is best accomplished by mixing partial waves of different symmetry. This provides a qualitative picture of why high-T_c materials (with large values of η) seem to be subject to covalent instabilities.

It has been repeatedly pointed out[41] that strong empirical evidence points to some special virtue in a cubic crystal structure. We suggest that cubic systems resist covalent instabilities. In all symmetry types except cubic, there is at least one structural parameter (such as c/a ratio) which can adjust without altering either volume or symmetry. As an example, hexagonal Be has a c/a ratio of 1.57, rather than the "ideal" value 1.63. The reason for the distortion is that at a slight cost in Madelung energy the lattice can adjust to maximize the size and effectiveness of the covalent band gaps, obtaining a large reduction in band-structure energy. If the symmetry were cubic, Be would probably have a lower melting point, higher $N(0)$, and higher λ and T_c. The cubic $A15$ structure frequently permits very high values of $N(0)$ which would probably not be stable in a system of lower symmetry. The coexistence of directional bonds and symmetry-stabilized large $N(0)$ may be the key features of high-T_c materials. This analysis of the benefits of cubic symmetry differs from the argument of Cohen and Anderson[35] based on umklapps.

To summarize, high-T_c superconductors are characterized by large values of λ (near 2) which occur in lattices which are relatively soft (in the sense that niobium has $M\langle\omega^2\rangle$ smaller by 2 than Mo). However, the increase in λ between a good superconductor like Nb and a very good one like Nb_3Sn comes more from an increase in η than a decrease in $M\langle\omega^2\rangle$. The benefit to T_c from increasing λ from 1 to 2 is 2.6 times greater if η is increased leaving $M\langle\omega^2\rangle$ fixed than if η is fixed and $M\langle\omega^2\rangle$ decreases. The available high-T_c materials probably represent cases where especially large values of η are possible.

ACKNOWLEDGMENTS

We thank R. Haydock, M. J. Kelly, C. M. M. Nex, W. E. Pickett, J. M. Rowell, J. C. Swihart, and E. Tosatti for helpful conversations, C. M. M. Nex for invaluable advice on computing, J. P. Garno for technical assistance, and M. L. Cohen for suggestions on the manuscript. One of us (P. B. A.) thanks A. B. Pippard for hospitality at the Cavendish Laboratory, which much of this research was carried out.

APPENDIX A: SOME PROOFS

To prove various properties of integrals of $\alpha^2F(\omega)$, it is convenient to define

$$g(\omega) \equiv (2/\omega\lambda)\alpha^2F(\omega) , \tag{A1}$$

so that $g(\omega)$ is a non-negative weight function normalized to unity on the interval $(0, \infty)$. Then the characteristic frequencies $\langle\omega^n\rangle$ are the moments of $g(\omega)$, and $\overline{\omega}_n$ denotes the nth root of $\langle\omega^n\rangle$. The properties we will prove are

$$\lim_{n\to 0} \overline{\omega}_n = \omega_{\log} \equiv \exp\int_0^\infty d\omega \ln\omega g(\omega) , \tag{A2}$$

$$\overline{\omega}_{n'} \geq \overline{\omega}_n \text{ for all } n' > n > 0 , \tag{A3}$$

$$f(a) \equiv \int_0^\infty d\omega\, g(\omega) \frac{\omega^2}{\omega^2 + a^2} \leq f_E(a) \equiv \frac{\langle\omega^2\rangle}{\langle\omega^2\rangle + a^2} . \tag{A4}$$

Property (A2) is almost trivial. We write $\overline{\omega}_n$ in the form

$$\overline{\omega}_n = \left(\int_0^\infty d\omega\, e^{n\ln\omega} g(\omega)\right)^{1/n} , \tag{A5}$$

and then expand the exponential for small values of $n\ln\omega$. Our weight functions $g(\omega)$ vanish above an upper frequency ω_c and are well behaved (i.e., do not diverge) at small ω. Therefore at very large or very small ω, where the first two terms in the expansion are a poor approximation, the contributions to the integral in (A5) are negligible. Thus for very small n we can write

$$\omega_n \cong \left(1 + n\int_0^\infty d\omega \ln\omega g(\omega)\right)^{1/n} . \tag{A6}$$

Then formula (A2) follows immediately from the well-known limit

$$\lim_{n\to 0} (1 + nx)^{1/n} = e^x . \tag{A7}$$

The proof of properties (A3) and (A4) will be based on a theorem quoted by Wheeler and Gordon.[42] We give her a special case of the general theorem, which deals with the problem of approximate evaluation of integrals over non-negative weight functions $h(x)$ for which a finite number of moments $\mu_0, \mu_1, \ldots, \mu_n$ are known. Let us suppose that the moments μ_0 and μ_1 are known and construct a δ function approximation $h_E(x)$ to $h(x)$ which has the same moments:

$$\mu_n = \int_0^\infty dx\, x^n h(x) , \tag{A8}$$

$$h_E(x) = \mu_0 \delta(x - \mu_1/\mu_0) . \tag{A9}$$

Then the theorem gives an estimate of the error involved in replacing h by h_E inside an integration, namely,

$$\int_0^\infty dx\, F(x)h(x) = \int_0^\infty dx\, F(x)h_E(x) + k^2 F^{(2)}(\xi) . \tag{A10}$$

In this theorem k^2 is a positive number which can be constructed from $h(x)$ (and vanishes only if $h = h_E$) and $F^{(2)}(\xi)$ is the second derivative of the integrating factor $F(x)$ evaluated at some (unspecified) point ξ in the range of integration. Theorem (A10) yields rigorous inequalities *provided* $F(x)$ has a second derivative of fixed sign in the range of integration.

We now use theorem (A10) to prove A3). Assume that $\overline{\omega}_n$ is known for some (fixed) value of n. Let us change variables and redefine the weight function

$$x = \omega^n , \qquad h(x) = \omega g(\omega)/nx . \tag{A11}$$

Then the first two moments of $h(x)$ are known:

$$\mu_0 = \int_0^\infty dx\, h(x) = \int_0^\infty d\omega\, g(\omega) = 1 ,$$

$$\mu_1 = \int_0^\infty dx\, xh(x) = \int_0^\infty d\omega\, \omega^n g(\omega) = \langle \omega^n \rangle = \overline{\omega}_n^n .$$

Then we can construct a δ-function approximation to $h(x)$,

$$h_E(x) = \delta(x - \langle \omega^n \rangle) . \tag{A12}$$

Now consider an integrating factor $F(x) = x^\alpha$, where α is assumed positive. The second derivative $F^{(2)}(\xi)$ is positive or negative depending on whether α is greater or less than 1. Thus from theorem (A10) we have the inequalities

$$\int dx\, x^\alpha h(x) \begin{cases} \leqq \int dx\, x^\alpha h_E(x) & \text{if } \alpha > 1 \\ \geqq \int dx\, x^\alpha h_E(x) & \text{if } \alpha < 1 . \end{cases}$$

Using the definitions of x, $g(x)$, and $g_E(x)$, these inequalities translate into

$$\langle \omega^{\alpha n} \rangle \begin{cases} \leqq \langle \omega^n \rangle^\alpha & \text{if } \alpha > 1 \\ \geqq \langle \omega^n \rangle^\alpha & \text{if } 0 < \alpha < 1 . \end{cases}$$

Finally, taking the $1/n\alpha$ power of these inequalities, theorem (A3) is proved.

Using very similar methods, theorem (A4) can be proved in a more general form, namely,

$$\int d\omega\, g(\omega) \frac{\omega^2}{\omega^2 + a^2} \leqq \frac{\langle \omega^n \rangle^{2/n}}{\langle \omega^n \rangle^{2/n} + a^2} , \tag{A13}$$

valid for $n \geqq 2$. All of the inequalities mentioned here become exact equalities *only* if $g(\omega)$ is a δ function. Thus the inequality (A13) would lead to a more general theorem on T_c than the one given in the text; namely, given λ, μ^*, and $\overline{\omega}_n$ for an arbitrary value $n \geqq 2$, the maximum T_c consistent with these parameters is obtained when (and only when) $\alpha^2 F$ is an Einstein spectrum. For simplicity we will give the proof only for $n = 2$ on the grounds that $\langle \omega^2 \rangle$ is the most "physical" moment of $\alpha^2 F$. We make the transformation (A11) for the case $n = 2$ to rewrite $f(a)$ [as defined in A4)]:

$$f(a) = \int_0^\infty dx\, g(x) \left(\frac{x}{x + a^2} \right) ,$$

$$f_E(a) = \int_0^\infty dx\, g_E(x) \left(\frac{x}{x + a^2} \right) .$$

The integrating factor $x/(x + a^2)$ has a negative second derivative for all positive values of x. Thus (A4) is immediately proved using theorem (A10).

APPENDIX B: ASYMPTOTIC LIMIT OF BCS THEORY

It is often incorrectly supposed that BCS theory puts an upper limit of Θ_D on T_c. This conclusion follows from the famous equation

$$T_c = \frac{\Theta_D}{1.14} e^{-1/N(0)V} . \tag{B1}$$

However, Eq. (B1) is only a weak-coupling approximation to the BCS-model equation given below:

$$1 = N(0)V \int_0^{\Theta_D/2T_c} dx \frac{\tanh x}{x} , \tag{B2}$$

where $x = \epsilon/2k_B T_c$. If the coupling $N(0)V$ is large enough, it is clear that the limit of integration $\Theta_D/2T_c$ must be small because the integrand, $\tanh x/x$, is approximately unity. The asymptotic behavior of the BCS model is then

$$T_c \to \lambda \Theta_D/2 , \tag{B3}$$

where the coupling constant $N(0)V$ has been denoted λ. This result has not escaped notice,[43] but there are qualitative arguments for not taking it seriously. BCS theory is a weak-coupling theory based on a "reduced" Hamiltonian. "Renormalization" effects are omitted in the reduced Hamiltonian, and these are often thought to diminish the effective coupling constant from λ to $\lambda/(1 + \lambda)$. This replacement occurs in McMillan's equation, and is accurate if $\lambda < 1.5$. However, for very large coupling we have seen that McMillan theory breaks

down and Eliashberg theory gives $T_c \propto \lambda^{1/2}$. We suspect that the occurrence of $\lambda^{1/2}$ follows from the fact that the interaction Hamiltonian in Eliashberg theory scales as $\lambda^{1/2}$. [The effective electron-electron interaction $\lambda/N(0)$ is quadratic in the electron-phonon interaction $M_{kk'}$, which occurs in the true Hamiltonian.] In BCS theory, the Hamiltonian contains a direct electron-electron interaction scaling as $\lambda/N(0)$. It would not be completely surprising if the actual asymptotic behavior of such a theory (using the full, not reduced, Hamiltonian) where $T_c \propto \lambda$ as in the reduced theory.

---

*Alfred P. Sloan Fellow. Work supported in part by National Science Foundation Grant No. GH037925.

[1]W. L. McMillan, Phys. Rev. 167, 331 (1968).
[2]G. M. Eliashberg, Zh. Eksp. Teor. Fiz. 38, 966 (1960); 39, 1437 (1960)[Sov. Phys.-JETP 11, 696 (1960); 12, 1000 (1961)].
[3]J. Bardeen, L. N. Cooper, and J. R. Schrieffer, Phys. Rev. 108, 1175 (1957).
[4]D. J. Scalapino, J. R. Schrieffer, and J. W. Wilkins, Phys. Rev. 148, 263 (1966).
[5]W. L. McMillan and J. M. Rowell, in *Superconductivity*, edited by R. D. Parks (Marcel Dekker, New York, (1969).
[6]J. M. Rowell and R. C. Dynes, in *Phonons*, edited by M. A. Nusimovici (Flammarion, Paris, 1971), p. 150.
[7]R. C. Dynes, Solid State Commun. 10 615 (1972).
[8]P. B. Allen and R. C. Dynes, J. Phys. C 8, L158 (1975).
[9]C. S. Owen and D. J. Scalapino, Physica 55, 691 (1971).
[10]G. Bergmann and D. Rainer, Z. Phys. 263, 445 (1974).
[11]W. Kessel, Z. Naturforsch. A 29, 445 (1974).
[12]P. B. Allen, Solid State Commun. 12, 379 (1973).
[13]C. R. Leavens, Solid State Commun. 14, 37 (1974).
[14]A result equivalent to Eq. (25) has been derived by D. Rainer [Symposium on Superconductivity and Lattice Instabilities, Gatlinburg, Tenn., 1973 (unpublished)]. This and several other results of this paper were also derived independently by J. W. Garland (private communication).
[15]P. B. Allen, Technical Report No. 7, TCM Group, Cavendish Laboratory (unpublished). Copies are available on request from the secretary, TCM Group, Cavendish Laboratory, Madingley Road, Cambridge CB3 OHE, U. K. This computer program has been run successfully by S. G. Louie and M. L. Cohen, who have also verified the program by producing identical results for T_c in a somewhat different way (private communication).
[16]C. R. Leavens and J. P. Carbotte, J. Low Temp. Phys. 14, 195 (1974). See especially Fig. 4 and the sentence directly underneath.
[17]J. C. Swihart, in *Proceedings of the Tenth International Conference on Low Temperature Physics* (Viniti, Moscow, 1967), Vol. II B, p. 275.
[18]P. Trofimenkoff and J. P. Carbotte, Phys. Rev. B 1, 1136 (1970).
[19]C. R. Leavens, Solid State Commun. 15, 1329 (1974).
[20]J. M. Rowell and W. L. McMillan, Phys. Rev. Lett. 14, 108 (1965).
[21]W. N. Hubin and D. M. Ginsberg, Phys. Rev. 188, 716 (1969).
[22]V. L. Ginzburg and D. A. Kirzhnits, Phys. Rep. 4, 343 (1972).
[23]D. A. Kirzhnits, E. G. Maksimov, and D. I. Khomskii, J. Low Temp. Phys. 10, 79 (1973).
[24]C. R. Leavens, Solid State Commun. 13, 1607 (1973). The quantity $\omega_0 e^{-\bar{\lambda}/\lambda}$ of this reference is closely related to $\omega_{\log}$ of the present paper.
[25]L. Y. L. Shen, Phys. Rev. Lett. 24, 1104 (1970).
[26]J. W. Garland, Phys. Rev. Lett. 11 111 (1963); 11, 114 (1963).
[27]J. H. Weaver, D. W. Lynch, and C. G. Olson, Phys. Rev. B 7, 4311 (1973).
[28]J. J. Hopfield, Phys. Rev. 186, 443 (1969).
[29]G. D. Gaspari and B. L. Gyorffy, Phys. Rev. Lett. 28, 801 (1972).
[30]R. Evans, G. D. Gaspari, and B. L. Gyorffy, J. Phys. F 3, 39 (1973).
[31]S. T. Chui, Phys. Rev. B 9 2097 (1974); 9, 3300 (1974).
[32]R. Gomersall and B. L. Gyorffy, Phys. Rev. Lett. 33, 1286 (1974).
[33]R. C. Dynes and J. M. Rowell, Phys. Rev. B 11, 1884 (1975).
[34]S. C. Ng and B. N. Brockhouse, in *Neutron Inelastic Scattering* (IAEA, Vienna, 1968), Vol. I, p. 253.
[35]M. L. Cohen and P. W. Anderson, in *Superconductivity in d- and f-Band Metals*, edited by D. H. Douglass (AIP, New York, 1972), p. 17.
[36]W. Weber, Phys. Rev. B 8, 5093 (1973).
[37]R. E. Glover, S. Moser, and F. Baumann, J. Low Temp. Phys. 5 519 (1971).
[38]N. W. Ashcroft, Phys. Rev. Lett. 21, 1748 (1968).
[39]S. T. Inoue and J. Yamashita, J. Phys. Soc. Jpn. 35, 677 (1973).
[40]A. S. Cooper, E. Corenzwit, L. D. Longinotti, B. T. Matthias, and W. H. Zachariasen, Proc. Natl. Acad. Sci. USA 67, 313 (1970).
[41]B. T. Matthias, Physica 69, 54 (1973).
[42]J. C. Wheeler and R. G. Gordon, in *The Padê Approximant in Theoretical Physics*, edited by G. A. Baker, Jr. and J. L. Gammel (Academic, New York, 1970), p. 99.
[43]We thank J. C. Swihart for pointing this out.